Corresponding Author: Dr. Stavros Melachroinos, Ph.D

Corresponding Author's Institution: Stinger Ghaffarian Technologies

First Author: Stavros A Melachroinos, PhD

Order of Authors: Stavros A Melachroinos, PhD; Frank G Lemoine, PhD; Nikita P Zelensky, PhD; David D Rowlands, PhD; Scott B Luthcke, PhD; Oleg Bordyugov

Abstract: We compute a series of Jason-2 GPS and SLR/DORIS-based orbits using ITRF2005 and the std0905 standards (Lemoine et al. 2010). Our GPS and SLR/DORIS orbit data sets span a period of 2 years from cycle 3 (July 2008) to cycle 74 (July 2010). We extract the Jason-2 orbit frame translational parameters per cycle by the means of a Helmert transformation between a set of reference orbits and a set of test orbits. We compare the annual terms of these time-series to the annual terms of two different geocenter motion models where biases and trends have been removed. Subsequently, we include the annual terms of the modeled geocenter motion as a degree-1 loading displacement correction to the GPS and SLR/DORIS tracking network of the POD process. Although the annual geocenter motion correction would reflect a stationary signal in time, under ideal conditions, the whole geocenter motion is a non-stationary process that includes secular trends. Our results suggest that our GSFC Jason-2 GPS-based orbits are closely tied to the center of mass (CM) of the Earth consistent with our current force modeling, whereas GSFC's SLR/DORIS-based orbits are tied to the origin of ITRF2005, which is the center of figure (CF) for sub-secular scales. We quantify the GPS and SLR/DORIS orbit centering and how this impacts the orbit radial error over the globe, which is assimilated into mean sea level (MSL) error, from the omission of the annual term of the geocenter correction. We find that for the SLR/DORIS std0905 orbits, currently used by the oceanographic community, only the negligence of the annual term of the geocenter motion correction results in a -4.67 ± 3.40 mm error in the Z-component of the orbit frame which creates 1.06 ± 2.66 mm of systematic error in the MSL estimates, mainly due to the uneven distribution of the oceans between the North and South hemisphere.

Suggested Reviewers:

The effect of geocenter motion on Jason-2 orbits and the mean sea level

S A Melachroinos (1,2), F G Lemoine (1), N P Zelensky (1,2), D D Rowlands (1), S B Luthcke (1), O Bordyugov (1,2)

(1) Planetary Geodynamics Branch, NASA Goddard Space Flight Center, Greenbelt USA, Frank.G.Lemoine@nasa.gov
(2) SGT-Inc., Greenbelt, Maryland, USA, Smelachroinos@sgt-inc.com, stavros.melachroinos@nasa.gov

Abstract

We compute a series of Jason-2 GPS and *SLR/DORIS*-based orbits using ITRF2005 and the *std0905* standards (Lemoine et al. 2010). Our GPS and *SLR/DORIS* orbit data sets span a period of 2 years from cycle 3 (July 2008) to cycle 74 (July 2010). We extract the Jason-2 orbit frame translational parameters per cycle by the means of a Helmert transformation between a set of reference orbits and a set of test orbits. We compare the annual terms of these time-series to the annual terms of two different geocenter motion models where biases and trends have been removed. Subsequently, we include the annual terms of the modeled geocenter motion as a degree-1 loading displacement correction to the GPS and *SLR/DORIS* tracking network of the POD process. Although the annual geocenter motion correction would reflect a stationary signal in time, under ideal conditions, the whole geocenter motion is a non-stationary process that includes secular trends. Our results suggest that our GSFC Jason-2 GPS-based orbits are closely tied to the center of mass (CM) of the Earth consistent with our current force modeling, whereas GSFC's *SLR/DORIS*-based orbits are tied to the origin of ITRF2005, which is the center of figure (CF) for sub-secular scales. We quantify the GPS and *SLR/DORIS* orbit centering and how this impacts the orbit radial error over the globe, which is assimilated into mean sea level (MSL) error, from the omission of the annual term of the geocenter correction. We find that for the *SLR/DORIS std0905* orbits, currently used by the oceanographic community, only the negligence of the annual term of the geocenter motion correction results in a -4.67 ± 3.40 mm error in the Z-component of the orbit frame which creates 1.06 ± 2.66 mm of systematic error in the MSL estimates, mainly due to the uneven distribution of the oceans between the North and South hemisphere.

Key words: Jason-2, geocenter motion, GPS, *SLR/DORIS*, mean sea level error

1. Introduction

The origin of the International Terrestrial Reference System (ITRS) is defined to be the center of mass of the Earth system, including oceans, atmosphere and continental water (McCarthy and Petit 2004). Ideally, the origin of the International Terrestrial Reference Frame (ITRF), realization of the ITRS, to which the Jason orbits are referenced, should coincide with the mean center of mass (CM) of the entire Earth system (Blewitt 2003). Although, the realization of the reference frame, through the geodetic stations, centered

in the CM, and the separation from physical processes to which the stations are subject, is a coupled problem. For example, according to the principal of the conservation of momentum, the CM has to be a kinematic fixed point, invariant to terrestrial dynamic processes. However, the redistribution of masses in the Earth system causes geocenter motion and as such seasonal, annual and trend variations between the CM and the center of figure (geometric center of the outer surface of the solid Earth) of the solid Earth to which the actual ITRF is referenced for sub-secular time scales (Dong et al., 2003; Blewitt et al., 2001). Métivier et al. (2010) have found that global ice melting on the Earth can induce long-term displacements of the geocenter particularly along the Z-axis, toward the North Pole. They have calculated that the geocenter velocity can reach 0.7-0.8 mm/yr and is today most probably between 0.3 and 0.8 mm/yr. As such, for the purpose of accurate geodetic observations, having access to a nearly instantaneous geocenter is extremely important for those missions that can sense geocenter motions to some extent but are not good enough to measure it well independently (Wu et al., 2012). Furthermore, the CM is directly related to satellite orbital motion and so is the most appropriate choice to model satellite geodetic measurements (Fritsche et al. 2010), such as altimetry.

From the above, and given the required sea level infrastructure stability of 0.1 mm/yr (Cazenave et al. 2009), geocenter motion of the CM with respect to the CF, ideally, should also be included in the process of precise orbit determination (POD), which is based on the site crust-fixed coordinates of GPS, SLR, and DORIS stations. This movement can be thought of as a global degree-1 loading displacement correction to be applied to the crust-fixed coordinates of the tracking network in order to reference them to the CM of the whole Earth (Cerri et al. 2010). Hitherto, the lack of a community consensus on a geocenter model has not allowed the geocenter to be forward modeled as part of the Jason altimetry orbit standards (Cerri et al. 2010, Zelensky et al. 2010). Therefore, our motivation for this investigation arises from the fact that the realization of an orbital frame for altimetry centered in the CM plays a major role in the definition and calculation of the rates of global MSL rise.

There have been a number of approaches for the determination of the geocenter motion models such as: (1) by measuring the translation of a tracking network relative to the center of the geodetic satellite orbits – the "network shift or geometric approach"; (2) by observing the deformation of the solid Earth due to the surface mass load – the "degree-1 deformation approach" (Kang et al. 2009, Lavallee et al. 2006, Blewitt et al. 2001). Dong et al. (2003) suggest the degree-1 deformation approach produces more stable geocenter estimates. Geocenter estimates based on satellite laser ranging (SLR), have been previously reported by Chen et al. (1999). When compared to estimates based on combined atmosphere, ocean and hydrological model outputs, Chen et al. (1999) found general agreement at the annual period but little correlation at the monthly timescale.

Here, we use two most recent versions of geocenter models: (1) The UT/CSR RL04 monthly geocenter time-series from Cheng et al (2010), which is based on the "network approach". Cheng et al (2010) use SLR data from five geodetic satellites (LAGEOS 1& 2, Starlette, Ajisai and Stella) to estimate a 5x5 gravity field along with 3 geocenter parameters (Tx,Ty,Tz). (2) The Swenson et al (2008) time-series based on the "degree-1

deformation approach". The degree-1 terms of this model are estimated from a combination of data from the Gravity Recovery and Climate Experiment (GRACE) satellite mission and the modeled global atmospheric and oceanic effects to the Stokes coefficients.

The 1st question we try to answer in this investigation is which of the produced Jason-2 orbit frames based on the GPS or the *SLR/DORIS* data is more closely centered to the CM. For this purpose, we characterize the spurious signals contained in the translational parameters of the GPS and *SLR/DORIS* Jason-2 orbit origin. Then we concentrate our efforts to the centering of the North/South component. Following this investigation, the suitability of the geocenter motion models and their consistency when used by each geodetic POD approach, GPS or *SLR/DORIS*, is examined. Then the error in the MSL from the omission of the geocenter motion is evaluated.

2. Description of the Jason-2 orbit set

For the purposes of this investigation we compute the Jason2 precise orbits using a dynamic and a reduced-dynamic approach (Bertiger et al. 1994). The current GSFC Jason-2 dynamic and reduced-dynamic orbits have been computed with GEODYN (Pavlis et al. 2009) processing GPS (Table 1), and combined SLR (Pearlman et al. 2002, Urschl et al. 2007) and DORIS (Tavernier et al. 2006, Willis et al. 2010) data using the *std0905* standards outlined in Table 1 of Zelensky et al. (2010) and Table 7 of Lemoine et al. (2010). These standards include the GRACE-derived static gravity field EIGEN-GL04S1 (Lemoine et al. 2007), the GOT4.7 (Goddard Ocean Tide Model) dynamic tide model (update to Ray, 1999), forward modeling of atmospheric mass flux using ECMWF pressure data (Klinker et al. 2000), a GRACE derived time varying gravity model capturing the annual variation (Luthcke et al. 2006), updated ITRF2005 SLR and DORIS station coordinates using LPOD2005 (Ries, 2008, Luceri and Bianco 2007) and DPOD2005 (Willis et al. 2009) and updated GPS station coordinates and orbits using IGS05 (IGSMAIL-5447, Ferland and Bourrassa 2006). The GPS *std0905* standards are outlined in Table 1. The GPS constellation orbits are held fixed to the coordinate set generated from a least squares (LSQ) fit to the IGS05 sp3 orbits. The GPS station positions are held fixed to their IGS05 coordinates. The entire GPS antenna phase center and their associated variations map used are compatible with the IGS05 framework. In the GPS dynamic orbit solution (*gpsdyn*) once-per-revolution (OPR) along & cross-track accelerations parameters are included. For the *SLR/DORIS* dynamic orbits 1 OPR parameter is estimated every 24-h in a 24-h long arc. For the *gpsdyn* orbits OPR parameters are estimated every 15-h in a 30-h arc with six hrs of overlap between adjacent arcs (Melachroinos et al. 2011a). Most of the orbit error due to radiation pressure is characterized by an OPR signal (Zelensky et al. 2010). This signal is largely removed upon the estimation of empirical OPR acceleration parameters in the orbit solution (Colombo 1986). However, complex errors in the radiation pressure model interact with the estimated empirical OPR parameters to create errors largely in the X and Y, and to a smaller extent, to the Z components of the orbit with a draconitic period of 118-days (Zelensky et al. 2010). Any SRP mis-modeling is expected to have no effect in the annual variation of the Z-component origin.

139
140 Our GPS and *SLR/DORIS* orbit data sets span a period of 2 years from cycle 3 (July
141 2008) to cycle 74 (July 2010). Next, we compare our *gpsdyn* to the *SLR/DORIS* orbits
142 and the GPS-based reduced-dynamic (*gpsred*) orbits (Melachroinos et al. 2011b) for
143 internal validation purposes. Also for reasons of external validation we use a set of
144 reduced-dynamic orbits from JPL release-11a standards (*jpl11a*) (Bertiger et al. 2010). A
145 reduced-dynamic POD solution is based on the denser and geometrically stronger GPS
146 tracking data (Bertiger et al. 1994, Luthcke et al. 2003). In our *gpsred* implementation
147 OPR along & cross-track accelerations are estimated every 30 min with process noise
148 standard deviation of $1.0 \times 10^{-9} \, \text{m/s}^2$ and an exponential decay function with a correlation
149 time of 1hr (Table 1). As demonstrated in Melachroinos et al. (2011a) GSFC's *gpsdyn*
150 and *gpsred* orbits agree to within 1 cm radially with the SLR-DORIS orbits and those
151 computed from other analysis centers (JPL, ESA and CNES), thus satisfying the accuracy
152 requirement of 1 cm proposed by the oceanographic community (Cazenave et al. 2009).
153 Table 2 summarizes the orbit data sets and their associated acronyms used further in this
154 study.
155
156 **3. Spurious signals in the Jason-2 orbit origin**
157
158 Based on a GPS LEO tracking approach (Kang et al. 2009) we extract the Jason-2 orbit
159 frame translational parameters per cycle by the means of a Helmert transformation
160 between a set of reference orbits and a set of test orbits. As in Kang et al. (2009), our
161 GPS LEO tracking system consists of the GPS constellation orbits (fixed), the GPS
162 ground station network coordinates (fixed) and the GPS onboard Jason-2 receiver in low
163 Earth orbit. The set of reference orbits is chosen to be the *gpsdyn* orbits due to the
164 stronger ties to the force modeling. The dynamic technique provides an orbit mostly
165 governed by the dynamic modeling while the reduced dynamic technique provides an
166 orbit mostly tied to the tracking data. The set of test orbits are the *jpl11a*, *SLR/DORIS* and
167 *gpsred* orbits.
168
169 To a certain extent, the estimated orbits should follow the TRF origin, as this is defined
170 by the tracking stations, and for the GPS-based orbits, also by the GPS constellation
171 coordinates used. This will greatly depend from the techniques used in the POD
172 processing. In the case of the *gpsdyn* and *SLR/DORIS* orbits, the satellite dynamics are
173 constrained by physical models. The transition from satellite states at different
174 measurement times to the state at the solution epoch is furnished by integration of the
175 equations of motion, which are governed mostly by the forces (dynamics) acting on the
176 satellite over the time of interest. As such the *gpsdyn* and *SLR/DORIS* orbit should
177 supposedly be closer centered to the CM origin defined by the force modeling used in the
178 POD. In the case of the *gpsred* orbits, a dynamic and a kinematic tracking technique are
179 combined for the better elimination of errors related to force modeling. Essentially, the
180 *gpsred* orbits should be closer tied to the ITRF origin defined by the geometry of the
181 denser GPS tracking data. If we suppose that one of the orbits is centered in the CM and
182 the other in the CF, then the estimated translation parameters could represent in reality a
183 geocenter motion based on a geometric approach. An apparent advantage of the satellite
184 tracking approach to interpret the geocenter motion between CM and CF is that they

185 determine the absolute location of the CM with respect to the Earth's surface (Wu et al.
186 2012). For the purpose of clarity, and as Collilieux et al. (2009) mention, in the sub-
187 secular time scales that we focus on our investigation, we must keep one thing in mind:
188 we are only able to investigate possible translational variations (what we call "geocenter
189 motion") due to the inaccessible constant between CF and CM.
190

191 We perform a least squares spectral analysis on the time-series of the estimated
192 translational parameters. As previously stated, a 118-day signal is dominant in the X and
193 Y components with the largest amplitudes of 2.8 mm and 2.3 mm respectively (Fig. 1a
194 and 1b). Especially in the X-component the largest signal comes from the transformation
195 of the *gpsdyn* and *SLR/DORIS* dynamic orbits. The 118-day signal is the precise
196 draconitic (beta-prime) period for the Jason satellites and this result supports the earlier
197 discussion about the remaining orbit error due to solar radiation pressure (SRP) mis-
198 modeling by Cerri et al. (2010) and Zelensky et al. (2010).
199

200 Fig. 1c illustrates that in the Z-component the annual signature has the largest amplitude.
201 Other signals of lower amplitude appear at the 87-days and 112-days period but their
202 origin remains unclear. These signals are very close to the 4th and 3rd harmonics (87-days
203 and 117-days respectively) of the GPS draconitic year of 351 days (Schmid et al. 2007,
204 Ray et al. 2008). The largest annual signature results from the comparison of the *gpsdyn*
205 to the *SLR/DORIS* orbits. The comparison of the *gpsdyn* to the *jpl11a* orbits exhibits an
206 annual signature of smaller, but still, of non-negligible amplitude. This demonstrates the
207 presence of residual error in the annual frequency either in the *gpsdyn*, *SLR/DORIS* or
208 *jpl11a* orbits. Does this represent an annual motion between the orbit origins or is it only
209 related to a GPS SRP-induced orbit mis-modelling error, which usually causes orbit
210 variations at the GPS draconitic year of 351 days? For that purpose we use the *gpsred*
211 orbits since those are less sensitive, by definition, to any dynamic mis-modeling errors
212 (Melachroinos et al. 2011b). The comparison of the Z-component from the *gpsdyn* to the
213 *gpsred* orbits does not exhibit any significant signatures (magenta line of Fig. 1c),
214 especially in the annual term but also not in any other draconitic term. The orbit
215 differences in Figures 1a-1c do not show any SRP mis-modeling sensitivity in the Z-
216 component, but rather only sensitivity in the X and Y components of the *std0905 gpsdyn*
217 and the *SLR/DORIS* orbits, at the Jason-2 draconitic period of 118 days. Furthermore, it
218 seems that the *gpsred* and gpsdyn orbits both have consistent Z-centering. Thus, the 365-
219 days signature in the Z-component between the *gpsdyn*, *SLR/DORIS* and *jpl11a* orbits,
220 suggests that it is largely related to an annual motion of the orbit origin. The question that
221 we now need to answer is which of the orbits is more closely centered to the CM?
222

223 **4. The north/south centering of the Z-component**
224

225 In this section we examine the centering of the orbits and turn our attention to the North-
226 South behavior of the Z-component. As seen previously, the most significant peak of the
227 Jason-2 translational time-series, exhibits an annual signature in the Z-component. We
228 incorporated the 3-dimensionnal annual term from the geocenter motion models of
229 Swenson et al. (2010) and Cheng et al. (2010) inside the Jason-2 POD process (trends

230 and biases removed) as a correction to the a-priori position of the tracking stations
231 according to Dong et al. (2003):

233 $$X^{CM}(t) = X^{CF}(t) + X^{CM}_{CF}(t) \qquad (1)$$

235 Where

237 $$X^{CF}(t) = X^{CF}_0 + V^{CF}_0(t) + \sum_i DX^{CF}_i(t) \qquad (2)$$

238 Here $X^{CF}(t)$ is the observed position under a CF frame (ITRF), X^{CF}_0 and V^{CF}_0 are position,
239 velocity at reference epoch   , defined under the CF frame, $DX^{CF}_i(t)$ are various nonlinear
240 time-dependent deformations due to solid Earth tide, pole tide, ocean tide, mass loading
241 from atmosphere (not applied here), non-tidal oceans (not applied here), surface ground-
242 water (not applied here), and other local effects, $X^{CM}_{CF}(t)$ in this case is the time-dependent
243 degree-1 loading displacement correction from the annual fitted term of the two
244 geocenter models where any offsets and trends have been removed.

246 For the Z-component, a shift in the station coordinates from the geocenter correction does
247 not correspond exactly in an equivalent shift in the orbit frame due to the orbit
248 inclination. As such, if there is a shift *dz* introduced to all a priori coordinates of the
249 ground stations due to the annual term of the geocenter motion correction model, the Z-
250 component *Tz* of the orbit will be affected by (Morel and Willis, 2005):

252 $$Tz = k \times dz \qquad (3)$$

254 Where *k* is a linear transfer function.

256 At first, we apply the geocenter motion correction models only in the *SLR/DORIS*
257 tracking stations of the POD process according to equations (1) and (2). We then
258 compute the Helmert translational parameters between the *gpsdyn* and the *SLR/DORIS*
259 orbits. Next, an annual curve to each Z-component time-series is fitted and compared to
260 the annual fitted curves from Swenson et al. (2010) and Cheng et al. (2010). In the
261 comparison we also include the *jpl11a* and the *gpsred* orbits. Fig. 2a illustrates the annual
262 term of the Z-component (black line) by Swenson et al. (2010) and compares it to the Z-
263 components of the Helmert transformations between the reference orbit set (*gpsdyn*) and
264 the test orbits. The *SLR/DORIS* Z-component annual terms are plotted with and without
265 the annual term of the geocenter motion correction (blue and red). Fig. 2b compares only
266 the annual terms of the *SLR/DORIS* Z-component to the annual term by Cheng et al.
267 (2010). The Z-component annual amplitudes from the two models and each set of the
268 Jason-2 *SLR/DORIS* Helmert transformations are summarized in Table 3.

270 From the comparison of the *SLR/DORIS* orbits without the geocenter motion correction
271 to the *gpsdyn* orbits (blue line in Fig. 2a and 2b), we find that the amplitude of the Z-
272 component annual signature is 2.82 mm. After the introduction of the annual geocenter
273 motion correction from Swenson et al. (2010) and Cheng et al. (2010) in the POD process

of the *SLR/DORIS* orbits, the translational variations of the origin drop down in amplitude by 2.10 mm and 1.17 mm (red line in Fig. 2a and 2b) respectively. The reduction from the initial annual signature of 2.82 mm between the *SLR/DORIS* orbits and the *gpsdyn* orbits (Table 3), resulted by both geocenter models, represents 25 % of the Swenson et al. (2010) and 58 % of the Cheng et al. (2010) annual term. In this sense the Cheng et al. (2010) model performs the best in reducing the *SLR/DORIS-gpsdyn* origin translational variations. The total signal reduced with respect to the modeled annual geocenter motion correction is 39 % for both cases. As expected, both models propagate consistently as a correction in the POD process. These results suggest that the *SLR/DORIS* orbits are not centered in the CM, whereas, the *gpsdyn* orbits closely follow the CM origin consistent with the conservative force modeling as this is realized through the GPS POD processing of Jason-2. Furthermore, the 7-parameter transformation between the *gpsred* and *gpsdyn* orbits, demonstrates that both orbits sets have a very consistent Z-origin (magenta line in Fig. 2a). Someone would expect that the *gpsred* orbits would follow the CF as this is defined by the geometry of the denser GPS tracking data, which dominate the reduced dynamic technique. On the contrary the *gpsred* orbits do not demonstrate any significant Z-origin motion with respect to the *gpsdyn* orbits, which further supports the argument that both orbits are centered closer to the CM. The annual signature of the transformation between *jpl11a* and GSFC's *gpsdyn* orbits, (green line in Fig. 2a) exhibits amplitude of 1.66 mm. In section 3, we have shown the observed SRP error does not contribute to the annual signature between the *jpl11a* and *gpsdyn*. This fact leaves an open question for further investigation to whether the annual signal seen in the Z-component of 1.66 mm between the two Jason-2 GPS orbit sets from two different analysis centers is due to an inconsistency in the conservative force modeling of the two solutions (time-variable gravity field) or whether is due to an origin motion.

5. Geocenter motion and mean sea level

We have found that the orbit set more closely centered to the CM is the Jason-2 *gpsdyn* and *gpsred* orbits. Thus we have succeeded in answering the question opened in section 3. Despite their dynamic definition, the *SLR/DORIS* orbits are centered in the CF defined by the *SLR/DORIS* network. It's worth noticing that the *SLR/DORIS std0905* orbits used in this study is the official product currently released and used by the community for MSL estimations. As such, in this section we will characterize the errors in the MSL studies that would not be seen by the users of satellite altimetry data, when using GSFC's *gpsdyn* or *SLR/DORIS* orbits (based on the *std0905* standards), without *a priori* knowledge of the annual geocenter motion.

Primarily, we must be aware that errors in the southern hemisphere MSL estimates (which are differences between the satellite altitude, as this is provided by the estimated orbits, and the radar altimetry data) will have a larger effect due to their statistical over-representation in the radar observations (Morel and Willis 2005). As such, we expect that the errors due to the omitted annual geocenter motion over the southern oceans, will have a greater weight.

319 In order to characterize these errors and their propagation over the oceans, we perform
320 the Helmert tranformation between the orbits of the same technique, GPS or *SLR/DORIS*,
321 where in one of the solutions the annual term of the geocenter motion has been applied in
322 the POD process.
323
324 The amplitudes of the propagated signals in the Z-component are illustrated in Table 4.
325 The corrected for the geocenter motion *SLR/DORIS* orbits exhibit a noticeable annual
326 effect in the Z-component of 74 % and 81 % compared to each geocenter model. In the
327 *gpsdyn* orbits the annual geocenter correction propagates with a ratio of 16 % and 19 %
328 with respect to each model (Table 4). The resulted amplitudes are small. As the transfer
329 function of the origin error is different depending on the technique and processing
330 scheme, the difference between orbits will include a part, which is proportional to the real
331 geocenter motion. In the case of the *gpsdyn* orbits the resulted ratios are very small.
332
333 Looking at the geographical distribution of the amplitudes of the radial orbit differences
334 in Fig. 3, we can note the asymmetry in the North-South direction over water when a land
335 mask is included. The amplitudes of the radial orbit error are significantly larger in the
336 case of the *SLR/DORIS* orbits and can reach 2.5 mm in high latitudes depending from the
337 model. The *gpsdyn* orbits suffer the least from the omission of the geocenter correction.
338 As the transfer function of the origin error is different depending on the technique and
339 processing scheme, the difference between orbits may include a part that is proportional
340 to the real geocenter motion. In the case of the *gpsdyn* orbits where the geocenter
341 correction has been applied, the resulted ratios are small. The above argument supports
342 the fact that the *gpsdyn* orbits are indeed centered closer to the CM. Those remain
343 practically insensitive to the geocenter motion correction introduced as a degree-1
344 loading displacement correction to the tracking stations. Which shows that the real
345 geocenter motion left in the GPS Jason-2 orbits is small since the transfer function
346 resulted after the transformation is also small (see Table 4).
347
348 Fig. 4 illustrates the phases of the geocenter motion correction as this propagates over the
349 globe into the orbit's radial component. Even though it is small, it worth noticing that the
350 GPS technique provides a geographical representation of the propagation of the geocenter
351 motion into the radial component, similar to the one from Blewitt et al. (2001).
352
353 Fig.5 represents the geographical distribution of the POD omission error on the MSL (in
354 mm) resulting from the geocenter motion model of Cheng et al. (2010) in the *SLR/DORIS*
355 stations for cycle 058 (Jan 28-Feb 07, 2010). The systematic error from the modeled
356 geocenter motion in the Jason-2 *SLR/DORIS* orbit frame results in a mean Z-component
357 of -4.67 ± 3.40 mm. This affects the MSL (DH) by 1.06 ± 2.66 mm (Table 5). The
358 systematic error in the Jason-2 *gpsdyn* orbit frame results in a mean Z-component of only
359 -0.83 ± 0.28 mm which affects the MSL by 0.17 ± 0.37 mm. We calculated for both
360 Jason-2 *gpsdyn* and *SLR/DORIS* orbits and compared to previous studies, the functions
361 (ratios DH/Tz in Table 5) that would result from the Tz error in the orbit frame (and not
362 in the station's TRF), in an error in the MSL, due to the negligence of the geocenter
363 motion. In the case of Beckley et al. (2007), by taking into account k = 0.74 from
364 equation (4) of Morel and Willis (2005), the real Tz error in the TOPEX orbit frame

365 results into an orbit drift of 1.33 mm/yr resulting from a TRF drift of 1.8 mm/yr in the
366 stations due to the transition to ITRF2005 from ITRF2000 (Altamimi et al. 2007). This
367 propagates in a -0.26 ± 0.72 mm/yr error in the MSL, which provides a transfer function
368 of -0.20, following our approach. In Morel and Willis (2005) a Z shift of 10 mm in the
369 TRF stations is found to propagate linearly in the orbit frame Z-component by 74 % (=
370 0.74 mm/mm). Given our approach, the error in the Z-component of the orbit frame
371 resulting from the 10 mm shift would then be 7.4 mm, which results in an error of 1.21
372 mm in the MSL and a transfer function of -0.16. Our transfer function is closer to
373 Beckley et al. (2007) and differs by 0.05 only from the transfer function of Morel and
374 Willis (2005). It seems that all three results are consistent. We should point out that it is
375 the first time that the study of Morel and Willis (2005) has been verified by real case
376 scenarios. The tiny differences are probably related to the fact that both in Beckley et al.
377 (2007) and our investigation the geographical latitudes covered by the real orbit
378 inclination are not the same with the simulated case scenario analyzed by Morel and
379 Willis (2005).

380 Fig. 6 illustrates the observed geographical MSL trend resulting from the geocenter
381 motion model applied in the *SLR/DORIS* stations from Cheng et al. (2010) over Jason-2
382 cycles 001 to 074 (2 years). For the whole period of the *SLR/DORIS* orbits, the
383 negligence of just the annual term of the geocenter motion correction creates an apparent
384 MSL rise of 0.14 ± 0.35 mm/yr in 2 years. This is a very important result because if
385 orbits based on *SLR/DORIS* and GPS are used during the inter-mission calibration phases
386 of TOPEX/Poseidon, Jason-1, Jason-2 and future Jason-3 then the omission of the
387 geocenter motion correction could potentially affect the inter-mission calibration of the
388 altimeter data.

389 Finally, by editing the SLR weighted residuals after the application of the geocenter
390 motion correction we see a slight improvement with the annual term of the Cheng et al.
391 (2010) model over not using any geocenter motion in the *SLR/DORIS* orbits. For the
392 *gpsdyn* orbits the residuals remain unchanged.
393
394 All the above, in addition to the small improvement in the SLR weighted residuals,
395 demonstrate that the geocenter motion correction should be included as a standard in the
396 Jason-2 POD process.

397 **6. Conclusions**

398 In conclusion, we have characterized the spurious signals contained in the origin of the
399 Jason-2 orbits from an analysis of GSFC's *SLR/DORIS*-based and GPS-based dynamic
400 and a set of reduced-dynamic orbits. A 118-day dominant signal was found in the X and
401 Y components of the comparison *gpsdyn* to the *SLR/DORIS* orbits. The 118-day signal is
402 the precise draconitic (beta-prime) period for the Jason satellites and it is due to solar
403 radiation pressure (SRP) mis-modeling. This result is consistent to the analysis by
404 Zelensky et al. (2010). In the Z-component the annual signature has the largest amplitude.
405 Other signals of lower amplitude appear at the 87-days and 112-days close to the 4th and
406 3rd harmonics of the GPS draconitic year of 351 days (Schmid et al. 2007), but their
407 origin still remains unknown. We've shown that the comparison of the *gpsdyn* to the

SLR/DORIS orbits exhibits a large annual signal in the Z-component suggesting a motion of the origin between the two orbit sets. The *jpl11a* orbits (Bertiger et al. 2010) also exhibit an annual signature in Z when compared to the *gpsdyn* orbits but of smaller amplitude. This left an open question for further investigation with respect to the consistency in the force modeling and the origin of the two analysis centers GPS orbit sets.

We examined the centering of the *SLR/DORIS* orbits with respect to the *gpsdyn* orbits after the introduction of the annual geocenter motion as a degree-1 loading displacement correction in the stations. For the geocenter motion correction we have used two models from Cheng et al. (2010) and Swenson et al. (2010). After the introduction of the annual geocenter motion correction from Swenson et al. (2010) and Cheng et al. (2010) in the POD process of the *SLR/DORIS* orbits, the initial translational variations of the origin with respect the *gpsdyn* orbits, dropped down from 2.82 mm in 2.10 mm and 1.17 mm respectively. Furthermore, the 7-parameter transformation between the *gpsred* and *gpsdyn* orbits, demonstrated that both orbits sets have a very consistent Z-origin. Based on these facts, we have concluded that our *gpsdyn* orbits closely follow the CM consistent with our conservative force modeling, while the *SLR/DORIS* are centered closer to the origin of the ITRF, which is the CF for sub-secular scales. Moreover, our investigation suggests that any SRP mis-modeling error on Jason-2 is not responsible for the annual signature seen in the Z-component comparison between *jpl11a* and the GSFC's *gpsdyn* orbits. This fact left an open question of whether this annual signal is due to some difference in the POD modeling, such as the time variable gravity, or whether is due to an origin motion as is proven to be the case with GSFC's *SLR/DORIS* orbits.

We have characterized the errors that would be seen by the users of satellite altimetry data when using the *SLR/DORIS std0905*-based Jason-2 orbits without *a priori* knowledge of the geocenter motion. The *SLR/DORIS* orbits, in which the annuals term of the geocenter motion has been taken in to account, exhibited a noticeable annual effect in the Z-component of the orbit frame of 74 % and 81 % compared to each geocenter model. In the case of the *gpsdyn* orbits this effect was found to be only 16 % and 19 % respectively with insignificant amplitude. The *gpsdyn* orbits remained practically insensitive to the applied geocenter motion correction. We have depicted that in the case of the *SLR/DORIS* orbits the geographical amplitude of the mean radial orbit error (DH) is significantly larger and can reach 2.5 mm in the poles. Moreover, our transfer function that connects the error in the Z-component of the Jason-2 orbit frame, from the omission of the annual geocenter motion correction, to the MSL error of both the *gpsdyn* and *SLR/DORIS* orbits is closer to the transfer function re-calculated from the study of Beckley et al. (2007) and slightly differs from the one from Morel and Willis (2005). It is worth noticing that it is the first time where the study of Morel and Willis (2005) has been revisited with real case scenarios

In this study we addressed only the annual term of the modeled geocenter motion as a degree-1 loading displacement to the tracking stations that participate in the POD process. Indeed, seasonal geocenter motion results from mass transfer at the Earth's surface. We do model a big part of the degree-1 signal, but this is only a portion of the

454 degree-1 deformation since we also have associated deformation. The tracking network
455 displaces also because of higher degrees. Future work could focus on the forward
456 modeling of the seasonal displacements at the stations together with the complete
457 geocenter model correction.

459 We have found that the omission of just the geocenter annual term can contribute to an
460 apparent 0.14 mm/yr error in the MSL estimates in 2 years based on the std0905
461 SLR/DORIS orbits. However, although the annual term of the geocenter motion could
462 reflect a stationary signal in time, the whole geocenter motion is a non-stationary process
463 that includes secular trends. For example global ice melting on the Earth has been found
464 to induce long-term displacements of the geocenter particularly along the Z-axis, toward
465 the North Pole. Métivier et al. (2010) have calculated that the geocenter velocity can
466 reach 0.7-0.8 mm/yr and is today most probably between 0.3 and 0.8 mm/yr. Especially
467 in the last decade it seems that there's an increase in the geocenter velocity not superior
468 to 0.5 mm/yr. Since one of the main objectives in the present development of altimetry
469 MSL is stability at the 0.1 mm/yr level (Cazenave et al. 2009), it would be very
470 interesting to extend the current study to the whole period of Jason-1 and Jason-2 with a
471 complete geocenter motion correction. Our results have shown that the Jason-2 GPS and
472 *SLR/DORIS* orbits respond differently to the omission of an annual geocenter model in
473 the POD process. Hence, if orbits based on *SLR/DORIS* and GPS are used during the
474 intermission calibration phases (e.g. TOPEX vs. Jason-1; Jason-1 vs. Jason-2), then the
475 geocenter model omission error could potentially affect the intermission calibration of
476 altimeter data. We need to elucidate whether this conclusion still applies if other
477 techniques are used to process GPS data than the ones we have applied in this paper
478 using fixed and filtered IGS orbits, and GPS double differences on Jason-2.

488 **References**

490 Altamimi, Z., X. Collilieux, J. Le Grand, B. Garyt, and C. Boucher, 2007. ITRF2005: A
491 new release of the International Terrestrial Reference Frame based on time series of
492 station positions and Earth orientations parameters, J. Geophys. Res.,
493 doi:10.1029/2007JB004949, in press.
494 Beckley B D, F G Lemoine, S B Luthcke, R D Ray and N P Zelensky, 2007. A
495 reassessment of global and regional mean sea level trends from TOPEX and Jason-1
496 altimetry based on revised reference frame and orbits, Geophys. Res. Lett. 34,
497 L14608, doi:10.1029/2007GL030002

Bertiger, W. I., Bar-sever Y E, Christensen E J, et al. 1994. GPS precise tracking of TOPEX/POSEIDON: Results and implications, J. Geophys. Res., 99(C12), 24,449–24,464, doi:10.1029/94JC01171.

Bertiger W, Shailen D D, Dorsey A, Haines J B, Harvey N, Kuang D, Sibthorpe A, Weiss P J, 2010. Sub-Centimeter Precision Orbit Determination with GPS for Ocean Altimetry, Mar. Geod. 33(S1):363-378, doi:10.1080/01490419.2010.487800

Blewitt, G., 2003. Self-consistency in reference frames, geocenter definition, and surface loading of the solid Earth. J. Geophys. Res. 108 (B2), doi:10.1029/2002JB002290, Art. No. 2103.

Blewitt, G., D. Lavallée, P. Clarke, K. Nurutdinov, 2001, A New Global Mode of Earth Deformation: Seasonal Cycle Detected, Science vol 294, pp 2342-2345

Boehm J, Niell A, tregoning P, Schuh H, 2006. Global Mapping Function (GMF): a new empirical mapping function based on numerical weather model data. Geophys res Lett 33:L07304. doi:10.1029/2005GL025546

Boehm J, Heinkelmann R, Schuh H, 2007. Short note : a global model of pressure and temperature for geodetic applications. J Geod 81(10):679-683, doi:10.1007/s00190-007-0135-3

Cazenave, A. D.P. Chambers, P. Cipollini, L.L. Fu, J.W. Hurrell, M. Merrifield, S. Nerem, H.P. Plag, C.K. Shum, Josh Willis, 2010. "Sea Level Rise - Regional and Global Trends" in Proceedings of OceanObs'09: Sustained Ocean Observations and Information for Society (Vol. 1), Venice, Italy, 21-25 September 2009, Hall, J., Harrison, D.E. & Stammer, D., Eds., ESA Publication WPP-306, doi:10.5270/OceanObs09.pp.11

Cerri L, JP Berthias,WI Bertiger, BJ Haines, FG Lemoine, F Mercier, JC Ries, P. Willis, NP Zelensky, M Ziebart (2010), Precision Orbit Determination Standards for the Jason Series of Altimeter Missions, Mar Geodesy, 33(S1):379-418, doi:10.1080/01490419.2010.488966

Chen, J.L., Wilson, C.R., Eanes, R.J., Nerem, R.S., 1999. Geophysical interpretation of observed geocenter variations. J. Geophys. Res. 104 (B2), 2683–2690.

Cheng M, J Ries, B Tapley, 2010. Geocenter Variations From Analysis of SLR data, IAG Symp., 138, inpress

Collilieux, X., Altamimi, Z., Ray, J., van Dam, T., Wu, X., 2009. Effect of the satellite laser ranging network distribution on geocenter motion estimation. J. Geophys. Res. 114, Art. No. B04402.

Colombo O.L, 1986. Ephemeris errors of GPS satellites. Bull Geod, 60, 64-84

Dong, D., Yunck, T., Heflin, M., 2003. Origin of the international terrestrial reference frame. J. Geophys. Res. 108 (B4), Art. No. 2200.

Ferland R, Bourassa M, 2006. From Relative to Absolute Phase Center Calibration: The effect on the SINEX Products, presented at the International GNSS workshop "Near-Earth Navigation & Geodesy at ESOC, European Space Agency, Darmstadt, Germany. Available from <http://nng.esoc.esa.de/ws2006/session10.html>

Fritsche M, R Dietrich, A Rulke, M Rothacher, P Steigenberger, 2010. Low-degree earth deformation from reprocessed GPS observations, GPS Solut (2010) 14:165-175, doi: 10.1007/s10291-009-0130-7

Hedin A E, 1987. MSIS-86 thermospheric model. J. Geophys. Res. 92(A5), pp 4649-4662.

544 Kang, Z.G., Tapley, B., Chen, J.L., Ries, J., Bettadpur, S., 2009. Geocenter variations
545   derived from GPS tracking of the GRACE satellites. J. Geod. 83 (10), 895–901.

546 Klinker E, Rabier F, Kelly G, Mahfouf J F, 2000. The ECMWF operational
547   implementation of four-dimensional variational assimilation. Part III : experimental
548   results and diagnostics with operational configuration. Q. J. R. Meteorol. Soc. 126,
549   1191

550 Knocke P C, Ries J C, Tapley B D, 1988. Earth radiation pressure effects on satellites in:
551   Proceedings of the AIAA/AAS Astrodynamics Conference, Minneapolis, Minnesota,
552   pp. 577-586, August 15-17.

553 Lavallée, D. A., T. van Dam, G. Blewitt, and P. J. Clarke (2006), Geocenter motions
554   from GPS: A unified observation model, J. Geophys. Res., 111, B05405,
555   doi:10.1029/2005JB003784

556 Lemoine F G, N P Zelensky, D S Chinn, D E Pavlis, D D Rowlands, B D Beckley, S B
557   Luthcke, P Willis, M Ziebart, A Sibthorpe, J P Boy, V Luceri, 2010. Towards
558   development of a consistent orbit series for TOPEX, Jason-1, and Jason-2, Adv in
559   Space Res, doi:10.1016/j.asr.2010.05.007

560 Lemoine J M, Bruinsma S, Loyer S, et al, 2007. Temporal gravity field models inferred
561   from GRACE data. Adv Space Res 39 (10), 1620-1629,
562   doi:10.1016/j.asr.2007.03.062

563 Luceri V, Bianco G, 2007. The temporary ILRS reference frame : SLRF2005,
564   International Laser Ranging Service Fall Meeting, 24-28 September 2007, Grasse,
565   France. Available from
566   http://www.oca.eu/gemini/ecoles_colloq/colloques/ilrs2007/articles.php?lng=enandp
567   g=98.

568 Luthcke SB, NP Zelensky, DD Rowlands, FG Lemoine, TA Williams, 2003. The 1-
569   Centimeter Orbit: Jason-1 Precision Orbit Determination Using GPS, SLR, DORIS,
570   and Altimeter Data, Mar Geodesy, 26: 399-421, doi:10.1080/01490410390256727

571 Luthcke, S.B., Rowlands, D.D., Lemoine, F.G., et al., 2006. Monthly spherical harmonic
572   gravity field solutions determined from GRACE intersatellite range-rate data alone.
573   Geophys. Res. Lett 33 (2), L02402, doi:10.1029/2005Gl024846

574 McCarthy, D. D., G. Petit (Eds.), IERS Conventions (2003), IERS Tech. Note 32, Verlag
575   des Bundesamts fur Kartographie und Geodasie, Frankfurt am Main. 2004.

576 Métivier L, Greff-Lefftz M and Altamimi Z, 2010. On secular geocenter motion: The
577   impact of climate changes, Earth and Planet. Sc. Lett., 296, pp. 360-366,
578   doi:10.1016/j.epsl.2010.05.021

579 Melachroinos S A, F G Lemoine, N P Zelensky, D D Rowlands, C Deng, D E Pavlis, S B
580   Luthcke, S M Klosko, 2011a. Status of Precise Orbit Determination for Jason-2
581   using the GPS, SLR, & DORIS data at NASA/GSFC, paper presented at the
582   European Geosciences Union General Assembly, EGU2011-10409, Vienna, Austria,
583   Available at < presentations.copernicus.org/EGU2011-2697_presentation.pdf>

584 Melachroinos S A, F G Lemoine, N P Zelensky, D D Rowlands, S B Luthcke, D S Chinn,
585   S M Klosko, J Dimarzio, D E Pavlis, O Bordyugov, 2011b. Jason-2 systematic error
586   analysis in the GPS derived orbits, paper presented at the American Geosciences
587   Union General Assembly, G41B-0740, San Francisco, CA, USA. Available at <
588   http://agu-fm11.abstractcentral.com>

589 Morel L and P Willis (2005), Terrestrial reference frame effects on global sea level rise
590   determination from TOPEX/Poseidon altimetric data, Adv in Space Res,
591   doi:10.1016/j/asr.2005.05.113
592 Pavlis D E, Deng C, Poulose S et al., GEODYN Operations Manuals, Contractor Report,
593   SGT Inc., Greenbelt, Maryland, 2009
594 Pearlman M R, Degnan J J, Bosworth J M, 2002. The International Laser Ranging
595   Service, Adv Space Res 30 (2), 135-143,doi:10.1016/S0273-1177(02)00277-6
596 Ray J, Altamimi Z, Collilieux X, van Dam T, 2008. Anomalous harmonics in the spectra
597   of GPS position estimates. GPS solute. 12, 55-64, doi:10.1007/s10291-007-0067-7
598 Ray R D, 1999. A global ocean tide model from TOPEX/Poseidon altimetry: GOT99.2,
599   NASA TM-1999-209478, NASA Goddard Space Flight Center
600 Ries J C, LPOD2005: a practical realization of ITRF2005 for SLR-based POD in:
601   Presentation, OSTST, Nice, France, November 2008. Available at
602   <http://www.aviso.oceanobs.com/fileadmin/documents/OSTST/2008/oral/ries.pdf>
603 Schmid R, Steigenbeger P, Gendt G, Ge M, Rothacher M, 2007. Generation of a
604   consistent absolute phase center correction model for GPS receiver and satellite
605   antennas, J. Geod. 81 (12), 781-798, doi:10.1007/s00190-007-0148-y
606 Swenson S, D Chambers, J Wahr (2008), Estimating geocenter variations from a
607   combination of GRACE and ocean model output, JGR, vol. 113, B084410,
608   doi:10.1029/2007JB005338
609 Tavernier G, Fagard H, Feissel-Vernier M, 2006. The International DORIS Service:
610   genesis and early achievements. J. Geod. 80 (8-11), 403-417, doi:10.1007/s00190-
611   006-0082-4
612 Urschl C, Beutler G, Gurtner W, et al. 2007, Contribution of SLR tracking data to GNSS
613   orbit determination, Adv in Space Res., Vol. 39, Issue 10, p. 1515-1523 doi:
614   10.1016/j.asr.2007.01.038
615 Willis P, Ries J C, Zelensky N P, Soudarin L, Fagard H, Pavlis E C, Lemoine F G, 2009.
616   DPOD2005 : An extension of ITRF2005 for Precise Orbit Determination, Adv.
617   Space Res., 44(5), 535-544, DOI: 10.1016/j.asr.2009.04.018
618 Willis P, Fagard H, Ferrage P, 2010. The International DORIS Service (IDS): toward
619   maturity. Adv. Space Res. 45 (12), 1408-1420, doi:10.1016/j.asr.2009.11.018
620 Wu X, J Ray, T van Dam, 2012. Geocenter motion and its geodetic and geophysical
621   implications, J. Geodyn. 58, 44-61, doi:10.1016/j.jog.2012.01.007
622 Zelensky NP , FG Lemoine, M Ziebart, A Sibthorpe, P Willis, BD Beckley, SM Klosko,
623   DS Chinn, DD Rowlands, SB Luthcke, DE Pavlis, V Luceri, 2010. DORIS/SLR
624   POD modelling improvements for Jason-1 and Jason-2, Adv. in Space Res., Vol. 46,
625   Issue 12, p. 1541-1558, doi:10.1016/j.asr.2010.05.008
626
627
628
629
630
631
632
633
634

635   Table 1: GSFC Jason-2 GPS POD model standards: *std0905*

Reference Frame and displacement of reference points	
GPS	38 IGS05 (Ferland and Bourassa 2006) TRF stations
Tidal CoM and EOP	GOT4.7 (update to Ray, 1999); VLBI high frequency terms
Ocean Loading	GOT4.7 (update to Ray, 1999) all stations
Earth tide	IERS2003
EOP	IERS Bulletin A daily consistent with ITRF2005 (Altamimi et al. 2007)
Precession Nutation	IAU2000
Satellite surface forces and attitude	
Albedo/IR	Knocke-Ries-Tapley (1988)
Atmospheric drag	MSIS86 (Hedin, 1987)
Radiation pressure	8-panel, CR=0.916 (tuned)
Attitude	Quaternions
Tracking data and parameterization	
Tracking data	Double Difference LC iono-free tracking data, float ambiguities, fixed and filtered IGS sp3 orbits
Troposphere modeling	1/hr scale(wet+dry) troposphere (GMF (Boehm et al. 2006)/GPT (Boehm et al. 2007)-Hopfield) adjusted using 2 paths (1 station + 2 GPS s/c) during the POD
Parameterization	arc : 24+6 h long *gpsdyn* : drag 1/8hr, 2 OPR along&cross / arc *gpsred* : drag 1/arc, OPR along&cross/ 15 min, sigma =1.e-09, correl time =3600 sec
Antenna Reference	
GPS stations +	PCOs and PCVs : igs05.atx

satellites	JPL GPS antenna PCV map consistent with igs05.atx, Revised LC GPS antenna PCO offsets	636
GPS Jason-2		637
		638

639
640
641
642
643
644
645
646
647
648
649 Table 2: Description of the Jason-2 orbit solutions used in this study

POD name used in the text	Description
gpsdyn	GSFC's GPS dynamic
gpsred	GSFC's GPS reduced dynamic
*gpsdyn_com_csr_*	GSFC's GPS dynamic + Cheng et al. 2010 CoM correction
*gpsdyn_com_swn_*	GSFC's GPS dynamic + Swenson et al. 2008 CoM correction
SLR/DORIS	GSFC's *SLR/DORIS* dynamic
SLR/DORIS_com_csr	GSFC's *SLR/DORIS* dynamic + Cheng et al. 2010 CoM correction
SLR/DORIS_com_swn	GSFC's *SLR/DORIS* dynamic + Swenson et al. 2008 CoM correction
jpl11a	JPL's release-11a GPS reduced dynamic

650
651
652
653
654
655
656
657
658
659
660

661 Table 3: Z-component annual amplitudes (mm) from each geocenter motion model and
662 orbit transformations compared to the ratios of reduction in the annual signature to each
663 geocenter motion model and the *SLR/DORIS – gpsdyn* comparison.

Geocenter model	Annual Amplitude	Geocenter model applied	Ratio of the reduction to the *SLR/DORIS – gpsdyn* signal	Ratio of the reduction to each model
Swenson et al. 2010	1.85			
Cheng et al. 2010	4.24			
Helmert transformation (ref. orbit *gpsdyn*)	Annual Amplitude			
SLR/DORIS	2.82			
*SLR/DORIS*_com_swn	2.10	Swenson et al. 2010	25 %	39 %
*SLR/DORIS*_com_csr	1.17	Cheng et al. 2010	58 %	39 %

664

665

666 Table 4: Z-component annual amplitudes (mm) and ratios from each orbit solution after
667 the geocenter motion correction to each model

Helmert transformation	Ref. Orbit	Amplitude (mm)	Phase (degrees)	Ratio of the resulted signature to each model
gpsdyn_com_swn	*gpsdyn*	0.3	62.7	16 %
gpsdyn_com_csr	*gpsdyn*	0.8	4.9	19 %
*SLR/DORIS*_com_csr	*SLR/DORIS*	3.1	7.2	74 %
*SLR/DORIS*_com_swn	*SLR/DORIS*	1.5	64.3	81 %

668

669 Table 5: Effect observed on the derived mean sea level (DH) resulting from the Cheng et
670 al. (2010) geocenter motion correction in the *gpsdyn* and *SLR/DORIS* stations for Jason-2
671 cycle 058 (Jan 28-Feb 07, 2010)

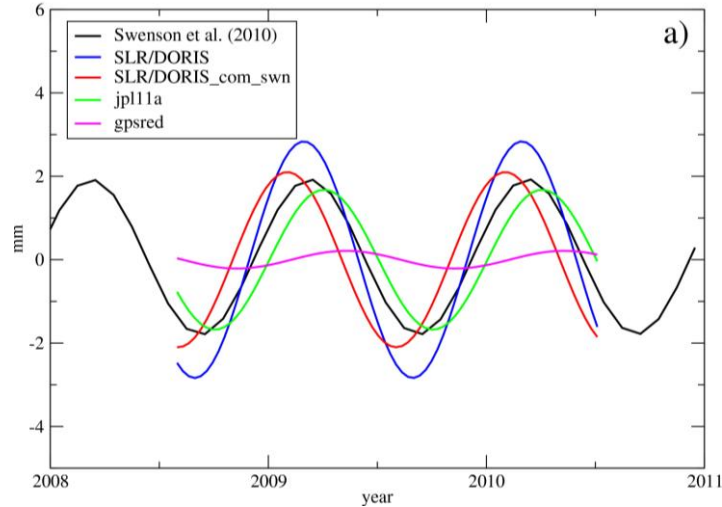| Orbit comparisons	Ref. Orbit	Tz (mm)	DH (mm)	DH/Tz
*SLR/DORIS*_com_csr	*SLR/DORIS*	-4.67 ± 3.40	1.06 ± 2.66	-0.22
gpsdyn_com_csr	*gpsdyn*	-0.82 ± 0.28	0.17 ± 0.37	-0.21

672

673

674

675

676
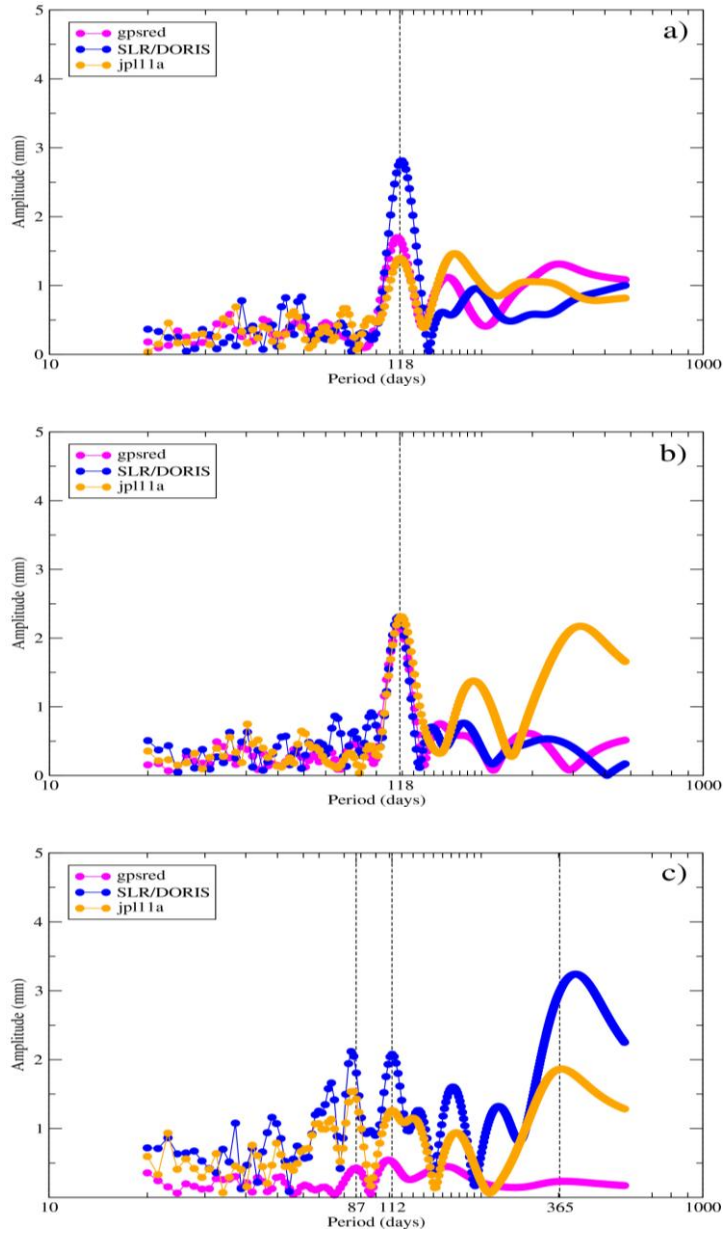
Figure 1: Periodogram (in mm) of the orbit origins after a 7-parameter Helmert transformation between the NASA GSFC Jason-2 GPS-based dynamic orbits and the three test orbits: NASA GSFC Jason-2 GPS-based reduced-dynamic (*gpsred*), NASA GSFC Jason-2 *SLR/DORIS dynamic* and JPL Jason-2 GPS-based reduced-dynamic (*jpl11a*). a) X-component, b) Y-component, c) Z-component. In purple, blue and orange are the comparisons to GSFC's *gpsred*, *SLR/DORIS* dynamic orbits and *jpl11a* GPS-based reduced dynamic orbits respectively.

684
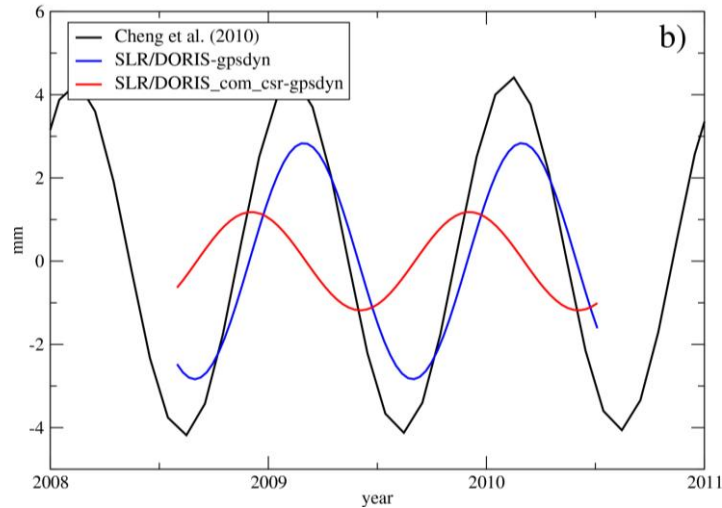
Figure 2: Jason-2 fitted annual signal of the Z-component time-series from the 7-parameter transformation between the *gpsdyn* (reference orbit) and the test orbits: *SLR/DORIS*, *jpl11a* and *gpsred*. a) compared to the Swenson et al. (2010) applied only in the *SLR/DORIS* orbits, b) compared to the Cheng et al. (2010) applied only to the *SLR/DORIS* orbits
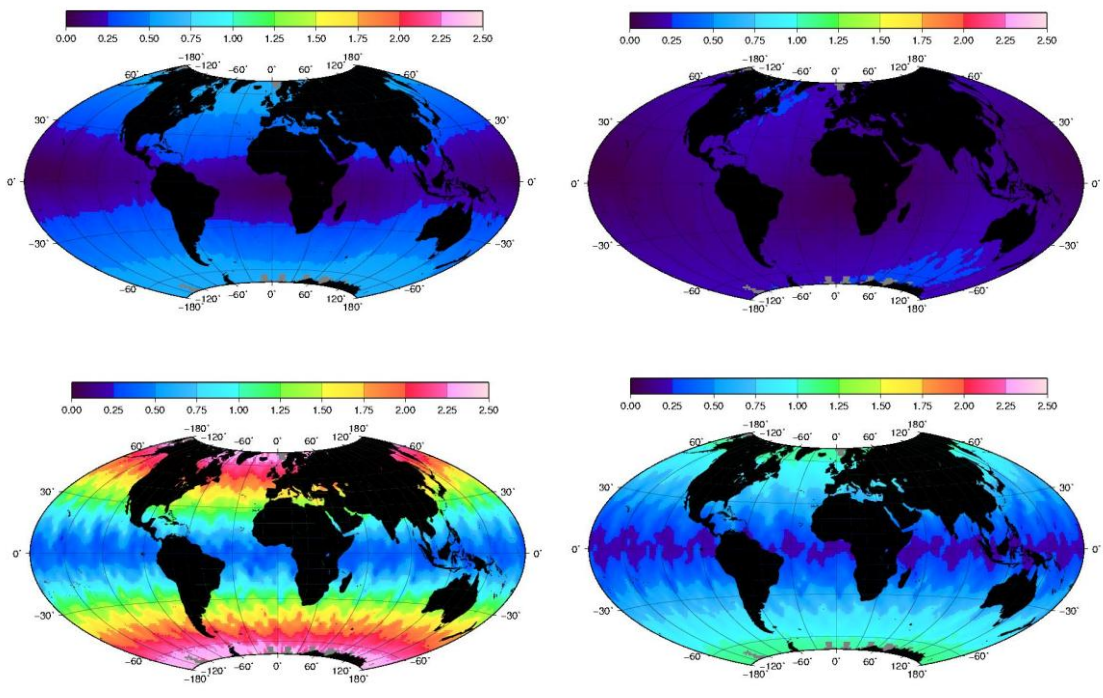
698

699
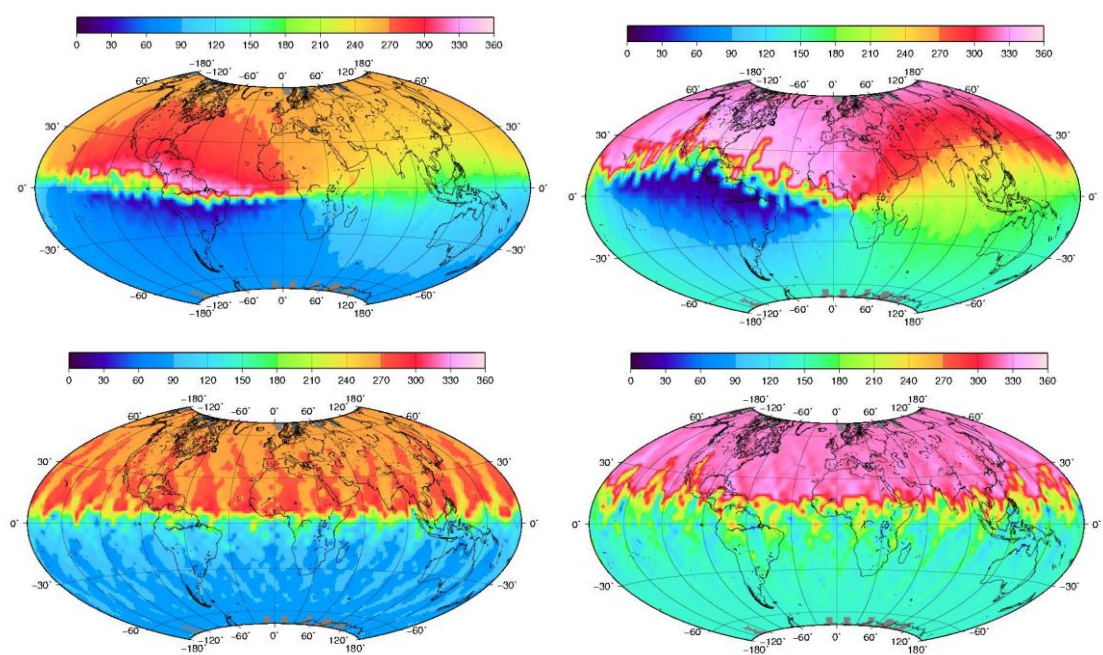
700 Figure 3: Amplitude (in mm) of the geocenter motion correction as it maps into the radial
701 orbit differences (DH) of the *gpsdyn* (up) and the *SLR/DORIS* (bottom) orbit frame. Left
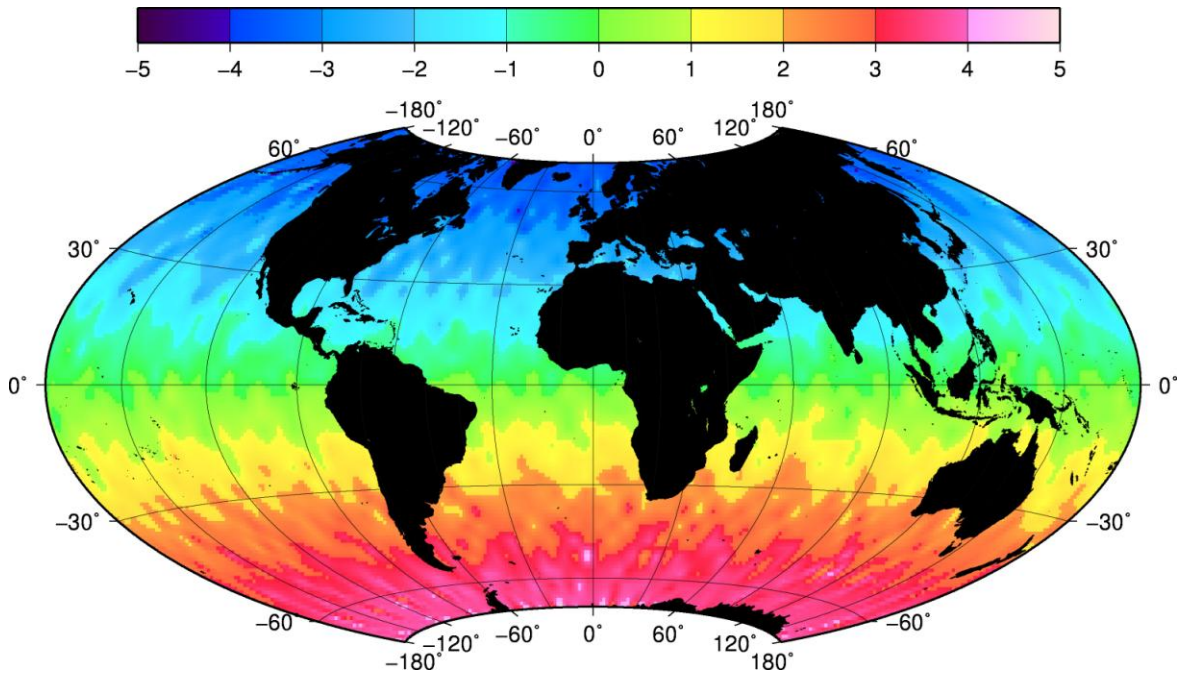702 from Cheng et al. (2010) and right from Swenson et al. (2010).

703

704
705 Figure 4: Phase (in degrees) of the geocenter motion correction as it maps into the radial
706 orbit differences (DH) of the *gpsdyn* (up) and the *SLR/DORIS* (bottom) orbit frame. Left
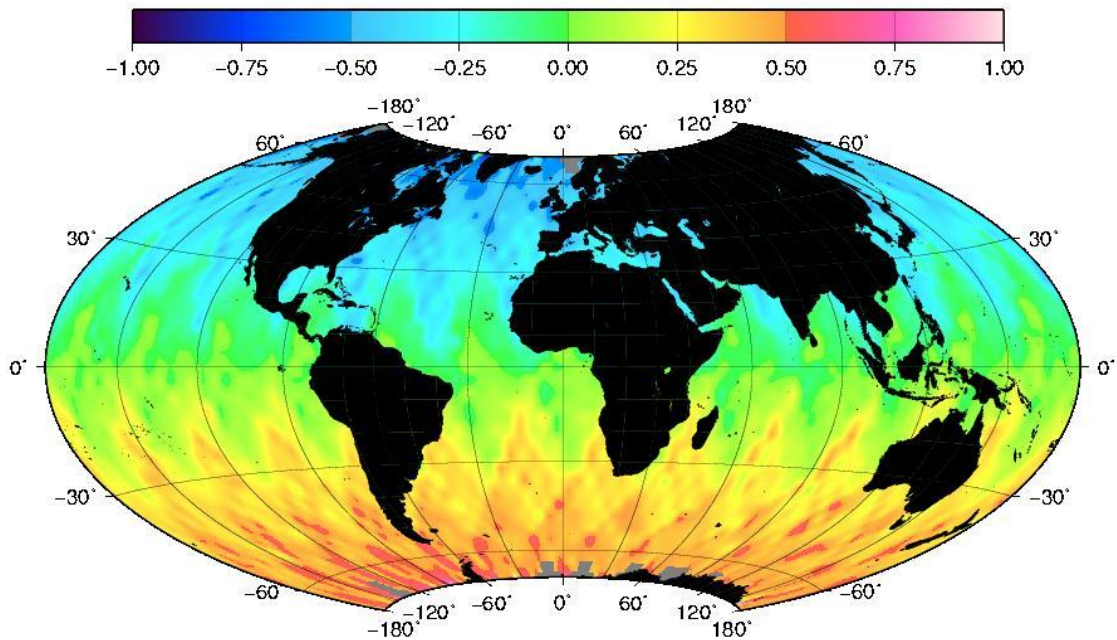707 from Cheng et al. (2010) and right from Swenson et al. (2010).

708

709
710

Figure 5: Observed geographical MSL error (in mm) resulting from the geocenter motion model of the *SLR/DORIS* stations from Cheng et al. (2010) for Jason-2 cycle 058 (Jan 28-Feb 07, 2010)

714

Figure 6: Observed geographical MSL trend (in mm/yr) resulting from the geocenter motion model of the *SLR/DORIS* stations from Cheng et al. (2010) over Jason-2 cycles 001 to 074 (2 years) : 0.14 ± 0.35 mm/yr

718

Rev. 1

While it appears necessary, as demonstrated in this paper, that geocenter motion should be applied in the POD process, so that all techniques provide orbits that are internally consistent, the authors may wish to consider (or pose to the altimetry community), whether the resulting orbits (presumably now properly centered at the CM) should in fact then be translated to the CF frame for purposes of computing sea level. The question arises since sea level is generally measured relative to the crust (e.g., tide gauges). Stated alternatively, should orbits used for sea level analysis really be in the CM frame or should they translated to the CF frame? This question would apply to the non-tidal as well as shorter period tidal geocenter motion.

Indeed, the reviewer is posing a very interesting and challenging question concerning modern and current geodetic sea-level investigations. Our future investigation is concentrating at exactly trying to answer to this question with 2 abstracts and one proposal recently submitted.
A tide gauge directly measures the displacement of the sea surface relative to a land point, and so would seem ideal. However the use of tide-gauge data alone to infer global measures of sea-level change is fundamentally problematic due to processes that intervene in the relative motions of the sea surface and the solid Earth on which the tide gauges are, over a broad range of spatial and temporal scales. The land beneath the tide-gauges is subject to motions such GIA (secular trends), coastal erosion, sedimentary loading, subsidence, atmospheric loading, tectonic processes and the different ocean/land response to present-day mass redistributions such as cryospheric loading and terrestrial hydrological loading. Another point is that the land motion near the costs on which the tide gauge are, provides a very poor sample distribution of the Earth deformation processes that will generally not average out on the global scale. Secondly, the vertical land motion from geodetic techniques used for the correction of the relative sea-level trends from the tide gauge sites, are subject to terrestrial reference frame errors. Also, an error in the terrestrial reference frame origin at the center of mass of the Earth implies an error in the height of sea surface inferred by satellite altimetry observations. Orbits whose origin is closer centered at the center of Mass of the Earth system, would ideally be insensitive to those reference frame realization errors. Tide gauges are immune to terrestrial reference frame errors only if the vertical velocities used for the correction of the relative sea level rates are inferred by other technique (cf. internal rates by G. Mitchum studies) and thus can be used only locally as the ground truth of calibration/validation for the satellite altimetry. In order though for these two types of sea-level observations to be comparable they need to be defined in the same ref. frame origin. For the tide gauges the origin is the center of the Solid Earth (CE) where as those of the satellite altimetry "ideally" is the center of mass of the Earth system (CM) defined by the satellite orbit dynamics. However the CE is never a frame of reference that can be realized by space geodesy. In GPS practice, for example, the CF frame is most commonly used. Also we must not forget that in order for the two types of

sea-level observations to be comparable, the vertical motions (from GPS heights normal to a geocentric ellipsoid) must be removed from the tide gauges records. So the way this vertical motion is defined is very important for the inter-comparisons, which means improved reference frames that for example would take into account seasonal mass redistribution, its effect on degree-1 deformation and therefore its effect on the frame origin, are needed.

Rev. 2

All suggested changes have been applied.